# Vehicle Stability Control of Heading Angle and Lateral Deviation to Mitigate Secondary Collisions

**Byung-joo Kim, Huei Peng**
**The University of Michigan**

G041 Lay Auto Lab, University of Michigan
Ann Arbor, MI 48109-2133
Phone: 1-734-647-9732
Fax: 1-734-647-9732
E-mail: bjukim@umich.edu

The objective of this study is to develop a post-impact vehicle stability control system that regulates both heading angle and lateral deviation from the original driving path, so that the severity of possible subsequent (secondary) crashes can be reduced. To characterize the vehicle motion after a crash event, an impact force estimation method and a vehicle motion prediction scheme are proposed. If the predicted unmitigated final heading angle is undesirable, and/or a large lateral deviation is expected, then proper differential braking and possibly steering action will be taken to drive the vehicle motion to a desired final state. Simulations and analysis results of the proposed state estimation and prediction algorithm will be evaluated, followed by the presentation on the proposed control algorithm.

Topics / Active Safety & Passive Safety, Integrated Chassis Control

## 1. INTRODUCTION

Motor vehicle accidents are one of the major societal problems the world is facing today. Approximately 5.5 million motor vehicle crashes were reported to the police during 2009 in the United States and about 33,000 persons were killed [1]. Some statistical studies [2-4] show that over 30% of all crashes have two or more harmful events following the initial collision. In about 70% of these multiple event crashes, the secondary harmful event is a collision with another vehicle. The remaining secondary events consist of collisions with fixed objects (23%), such as trees or utility poles, and rollovers (7%). It is also shown that risks of both injury and fatality increased with the number of collision events [2]. Moreover, A National Highway Traffic Safety Administration (NHTSA) crash analysis report for advanced restrained system [4], based on the data from 1988 to 2004, shows the vehicle spin angle distribution in the most harmful secondary event crashes by multiple impacts. As shown in Fig. 1, around 85% of the cases involved 90° turns to either clockwise or counter clockwise that caused results of high-risk secondary crashes. Since the sides of vehicles are more vulnerable than fronts and rears in terms of absorbing crash energy and shielding occupants, the risk of fatal and serious injury to occupants is estimated to be high. This report also shows that 53% of fatalities in the driver and front-seat passenger 13 years old or older were front to side impacts based on 2002-2006 Fatality Analysis Reporting System (FARS) crash databases.

To prevent and reduce vehicle crashes, various

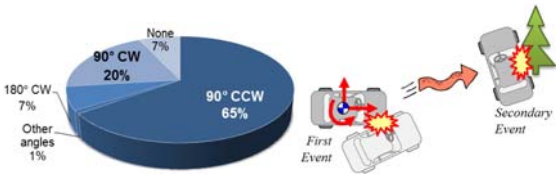


Fig. 1. Vehicle spin angle distribution of the most harmful secondary event crashes with multiple impacts. (CW: Clockwise, CCW: Counter clockwise) [4]

vehicle safety systems have been developed. Among them, the vehicle yaw stability control system, called Electronic Stability Control (ESC), has demonstrated positive effects on reducing single vehicle crashes [5, 6]. However, its effect on secondary crashes has not been fully analyzed. Since these control algorithms are not specifically designed to intervene after a vehicle-to-vehicle impact occurs, only limited control actions can be applied. Moreover, under typical high speed driving conditions, even a minor collision between vehicles can lead to devastating consequences if the driver fails to react properly. Hence, it is critical to actively maneuver the vehicle to avoid subsequent accidents or mitigate their severity. If the vehicle sensors and control actuators still function normally, there is a chance to stabilize the vehicle to counteract the undesired vehicle motion after an impact.

Using steering or braking actions after a minor collision has been studied in the literature. Chan et al. [7] developed a steering control system in a post-impact situation to stabilize the vehicle. Bosch introduced a

Secondary Collision Mitigation (SCM) safety feature linked with an airbag control unit as a part of their CAPS (Combined Active and Passive Safety) system [8]. Yang et al. [9, 10] proposed an optimization scheme using differential brake to minimize the maximum course deviation induced by an impact. And, Zhou et al. [11, 12] developed a control measure to mitigate vehicle post-impact skid and yaw motions from an external initial impact. Although these systems are able to stabilize yaw motion and minimize lateral deviation from the original course, the threat of a vulnerable heading angle to subsequent collisions with another moving vehicle or stationary object still exists. For example, if the vehicle is broadsided by another vehicle, the occupant may suffer more severe injury than the case with front or rear-end collisions.

The objective of this study is to design a vehicle motion stabilization system by predicting the heading angle induced by an external impact. The system can then control vehicle spin motion to reach a safe heading angle (0°, 180°, 360°, etc.) through proper activation of differential braking and possibly steering. It is envisioned that this system may help to reduce the probability of occurrence and severity of secondary crashes. The remainder of this paper is organized as follows. To predict a vehicle state after an impact, the strength of impact is predicted by a proposed algorithm presented in Section 2. The vehicle motion characteristics are investigated using simulation in Section 3. And possible control actions based on the optimization scheme are shown, and its effectiveness for vehicle motion is demonstrated in Section 4. Finally, conclusions and future work are drawn in Section 5.

## 2. IMPACT FORCE AND VEHICLE RESPONSE PROJECTION FROM CRASH EVENT

In this section, schemes for predicting the strength of the impact forces and vehicle response after the impact are proposed. The proper vehicle control action will then be determined based on the predicted vehicle motion. The algorithm is designed based on a few assumptions. First, the entire event is assumed to occur on a straight road, and only two vehicles (a bullet vehicle and a target vehicle) are involved in the collision. The sensors and steering/braking actuators in the target vehicle are assumed to be intact after the collision and function normally despite the collision.

After an impact, vehicle velocities and yaw rate may jump. From the algorithm shown in [11], a crash event can be detected in 3 time steps after the crash, using yaw rate and lateral acceleration signals and properly selected threshold values. The estimation of the strength of the impulse and the impact location is performed with vehicle dynamic transitional maneuvers. The overall process for predicting impact force and vehicle response after impact is shown in Fig 2. To start the control action as early as possible, the crash force prediction is performed before reaching the half-way point of the crash duration. Two impulse estimation steps are projected to the half-way duration point.

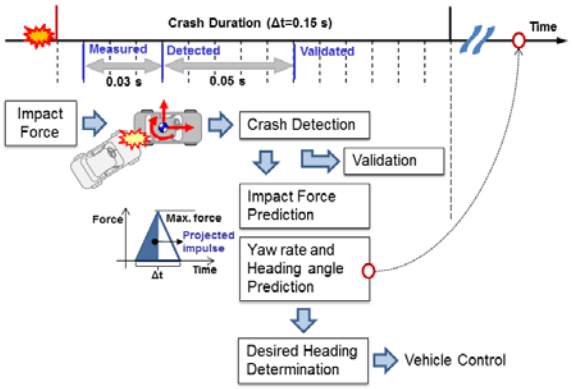


Fig. 2. Function diagram for impact force and vehicle motion prediction

Approximating the impact force by a triangular pulse with a known crash duration [13], this force profile can be predicted before the crash ends. Once the force profile is estimated, the vehicle response after impact is predicted using the 4DOF vehicle model derived in [11].

### 2.1 Impact Force Prediction Model

Once the impulse profile is estimated, the magnitude and the location of the impulse can be computed by using a crash dynamics model and the measured vehicle states. The model includes the equations of motion in the longitudinal, lateral, yaw and roll degrees of freedom, approximated to the discrete time in a trapezoidal form [11]. The strengths of the impulse and its location in the x-y plane are then inferred from equation (1)-(3).

$$P_x = M\cdot\left(V_x - v_x\right) - M\frac{\Delta t}{2}\left(V_y\Omega_z + v_y\omega_z\right) \tag{1}$$

$$P_y = M\cdot\left(V_y - v_y\right) + M\frac{\Delta t}{2}\left(V_x\Omega_z + v_x\omega_z\right) - m_R h\cdot\left(\Omega_x - \omega_x\right) + \frac{\Delta t}{2}C_f\left(\frac{V_y + a\Omega_z}{V_x} - \frac{v_y + a\omega_z}{v_x}\right) + \frac{\Delta t}{2}C_r\left(\frac{V_y - b\Omega_z}{V_x} - \frac{v_y - b\omega_z}{v_x}\right) \tag{2}$$

$$P_y x_A - P_x y_A = I_{zz}\left(\Omega_z - \omega_z\right) + I_{xz}\left(\Omega_x - \omega_x\right) + \frac{\Delta t}{2}aC_f\left(\frac{V_y + a\Omega_z}{V_x} - \frac{v_y + a\omega_z}{v_x}\right) - \frac{\Delta t}{2}bC_r\left(\frac{V_y - b\Omega_z}{V_x} - \frac{v_y - b\omega_z}{v_x}\right) \tag{3}$$

The right-hand sides of the three equations above are assumed to be known from vehicle sensor measurements, vehicle parameters, and collision time duration. There are four unknown quantities on the left hand side of the equations: strengths of the impulse in the x and y direction ($P_x$ and $P_y$), and the location ($x_A$ and $y_A$). To solve the 4 unknown variables based on the three equations, the following strategy is used: If one of the impact location parameters ($x_A$, $y_A$) is less than the geometric maximum value, then the other one should be fixed at its maximum. So, the equations are calculated twice, assuming that the impact location is either on the side of the vehicle or on the rear bumper. Only the answer that is geometrically plausible is taken as the solution. Linear extrapolation is then used to project impulses ($P_x$, $P_y$) at the half-way point of the

crash time duration. Assuming that the impulse profile is an isosceles triangle, the projected impulse will be half of the area of the triangle. The impact force ( $F_x$ , $F_y$ ) is then predicted by evaluating the maximum height of the impulse profile.

### 2.2 Vehicle Motion Prediction Model

The calculated impact force is used to predict the vehicle motion. The 4DOF vehicle dynamics model in [11] is used which accounts for vehicle motion and tire forces induced by external forces,

$$M(\dot{v}_x - v_y\omega_z) = F_x \tag{4}$$

$$M(\dot{v}_y + v_x\omega_z) - m_R h\dot{\omega}_x = F_y + F_{yf} + F_{yr} \tag{5}$$

$$I_{zz}\dot{\omega}_z + I_{xz}\dot{\omega}_x = x_A F_y - y_A F_x + aF_{yf} - bF_{yr} \tag{6}$$

$$I_{xxs}\dot{\omega}_x + I_{xz}\dot{\omega}_z - m_R h(\dot{v}_y + v_x\omega_z) = F_y(z_A - h) + (m_R gh - K_s)\phi - D_s\omega_x \tag{7}$$

where $M$ is the vehicle mass, $v_x$ is the vehicle forward speed, $v_y$ is the vehicle lateral speed, $\omega_z$ and $\omega_x$ are the yaw rate and roll rate, $F_x$ and $F_y$ are impact forces, $F_{yf}$ and $F_{yr}$ are the lateral tire force at the front and rear axles, respectively.

In the post-impact scenarios analyzed in this paper, the vehicle side slip angle varies in a very wide range. The typical range of side slip angle considered in ESC applications is around -30 to 30 degrees [14]. In this study, it is necessary to track a much wider range of side slip angle, up to 360 degrees. Fig. 3 shows the Magic Formula tire model [15] for combined longitudinal and lateral forces as functions of the tire side slip angle and the longitudinal slip ratio ( $\lambda$ ).

Note that tire forces are displayed along a full circle range of angles. The interesting regions are near the multiples of 180 degree angles including the zero degree. Around the regions, especially when $|\lambda|$ is small, the directions (or sign) of lateral forces are significantly changed within the very narrow range of sideslip angles. It can be easily estimated that the combinations of different force directional changes in each tire generate a certain amount of yaw moment on the car. This will be discussed with the simulation analysis in the following subsection.

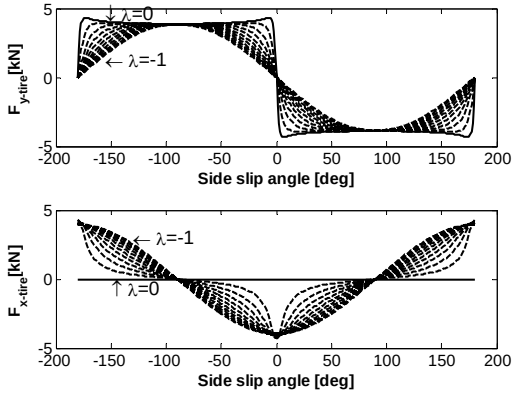


Fig. 3. Lateral and longitudinal forces of a tire model as functions of the side slip angle ( $\lambda$ : Longitudinal slip ratio)

### 2.3 Analysis of Vehicle Spinning Motion

In this subsection, vehicle motion is evaluated to figure out the trajectory of a spun vehicle after an external impact. Simulation are performed using the commercial software CarSim with the build-in template parameters corresponding to the "Baseline big SUV" (M=2450kg, a=1.105m, b=1.745m) [16]. It is assumed that the vehicle is traveling with an initial longitudinal speed of 29m/s and zero initial lateral speed, yaw rate, and roll rate. The collision impact lasts for 0.15 seconds with the sine square force profiles, and the impact location is 0.1m to the left of the center of the rear bumper. The road is assumed to be flat and straight, and its adhesion is assumed to be homogeneous with frictional coefficient $\mu = 0.7$ . Fig. 4 shows the vehicle motion induced by the crash impact without any mitigating driving, braking, or steering control actions.

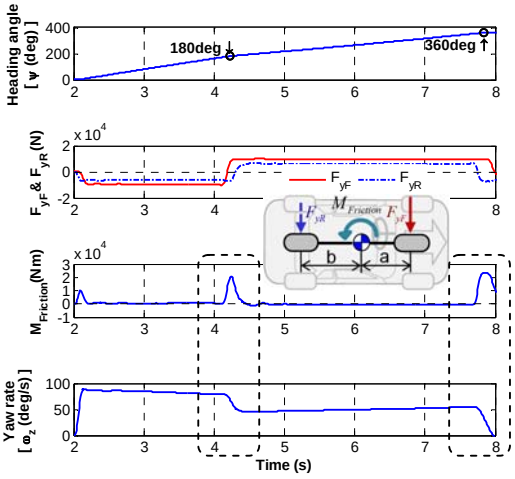


Fig. 4. Simulated vehicle motion after a collision

Let $F_{yf}$ and $F_{yr}$ to denote the tire lateral forces at the front and rear axles, respectively. $M_{Friction}$ is the induced yaw moment calculated from the tire lateral forces, then we have

$$M_{Friction} = a \cdot F_{yF} - b \cdot F_{yR} \tag{8}$$

This induced moment acts as a counter reaction against the moment from the collision impact and shows remarkable effects when the vehicle heading angle crosses 180° and 360°. As shown in the tire model (Fig. 3), lateral force changes with slip angle quickly around 0° or multiples of 180° angles, especially when tires are rolling ( $\lambda = 0$ ). Since the lateral forces of the front and rear tires switch signs at slightly different time (due to the fact the distances from the center of gravity to the axles are different), this transitional phase introduces large yaw moment when the lateral forces at the two axles are of opposite signs. Therefore, the yaw rate is significantly reduced when the vehicle heading angle crosses through 180° and 360°.

### 2.4 Prediction Results

The proposed impulse estimation and vehicle motion estimation algorithms are validated using Carsim simulations in Fig. 5.

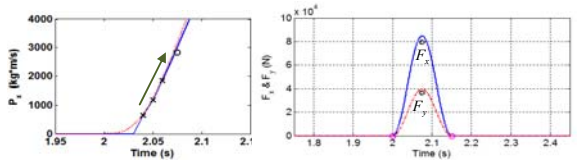


Fig. 5. Comparison of actual and projected impulse and impact forces ('o' represents the projection point)

The impact starts at 2 seconds and the impulse is estimated with measured signals and the equation of motion in subsection 2.1. The linearly extrapolated result from the impulses estimated from three measurements projects the impulse at the half-way point of the crash duration. And the predicted forces are obtained by calculating the height of the assumed triangle with an area that is twice the size of the projected impulse magnitude. The predicted vehicle dynamic response to the projected impact forces is shown in Fig. 6.

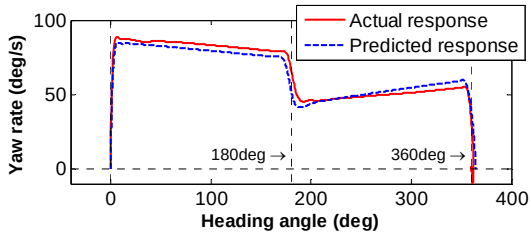


Fig. 6. Comparison of actual and predicted response of the struck vehicle

The yaw rate peaks at 89°/s and the vehicle keeps spinning and drops quickly at each 180° crossover. The prediction results seem to be accurate enough to be used for control interventions.

## 3. VEHICLE TRAJECTORY STUDY

Based on the predicted vehicle motion, the desired final heading angle can be determined. The hypothesis is that it will be beneficial to reach a final heading angle of 180° or 360° (or multiples of 180° thereafter) with respect to the lanes to avoid side impact from another bullet vehicle, and to avoid large lateral displacement so that the vehicle does not encroaching excessively into the adjacent lanes. Once the final heading angle is identified, control actions will then be computed to stabilize vehicle motions to the desired heading angle.

### 3.1 Vehicle Model in the Global Coordinate

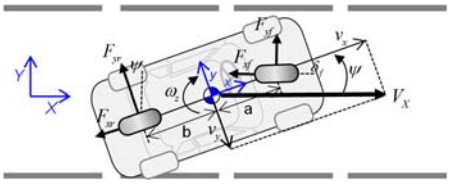

Fig. 7. Top view of the vehicle in the global coordinate

Since the relative motion of the vehicle with respect to the road is of interest, the motion vectors need to be transformed into the global coordinate system as shown in Fig. 7:

$$\dot{V}_X = \frac{(F_{xf} + F_{xr}) \cdot \cos\psi - (F_{yf} + F_{yr}) \cdot \sin\psi}{m} \tag{9}$$

$$\dot{V}_Y = \frac{(F_{xf} + F_{xr}) \cdot \sin\psi + (F_{yf} + F_{yr}) \cdot \cos\psi}{m} \tag{10}$$

$$v_x = V_X \cos\psi + V_Y \sin\psi \tag{11}$$

$$v_y = -V_X \sin\psi + V_Y \cos\psi \tag{12}$$

where ψ is the heading angle, the angle between the vehicle centerline and the road tangent line, and $\delta_f$ is the front wheel steering angle. The coordinate system (X, Y) is fixed on the ground, serving as a frame of reference for vehicle motion on the road. The body fixed coordinate system is denoted by (x, y) with its origin located at the center of gravity (CG) of the vehicle. To track the side slip angle even at magnitudes above 90°, the longitudinal and lateral velocity vectors in vehicle coordinates are determined by the velocities in the global coordinates and heading angles during spinning. The vehicle side slip angle ($\beta$) and tire side slip angles ($\alpha_f, \alpha_r$) are determined from the following equations:

$$\beta = atan2(v_y, v_x) \tag{13}$$

$$\alpha_f = atan2\left(\left(v_y + a \cdot \omega_z\right), v_x\right) - \delta_f \tag{14}$$

$$\alpha_r = atan2\left(\left(v_y - b \cdot \omega_z\right), v_x\right) \tag{15}$$

where *atan2* is the four-quadrant inverse tangent function that produces results in the range (-π, π]. To avoid singularities of this calculation, the magnitude of longitudinal velocity ($v_x$) is limited when it is near zero [14]. In addition, lateral vehicle position during spinning is obtained by integrating the lateral velocity in the global coordinate system.

### 3.2 Vehicle Motion Analysis with Brake Action

As shown in the tire model (Fig. 3), longitudinal and lateral forces are functions of side slip angles and longitudinal slip ratios of the individual tire. The simulation results in this subsection show that the combination of tire forces generates different vehicle yaw motions.

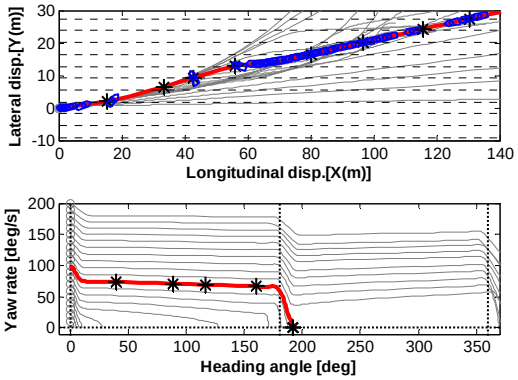


Fig. 8. Projected vehicle position and motion without any mitigating brake action (*: indicates lane boundary crossing)

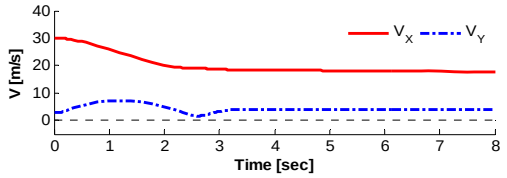


Fig. 9. Directional vehicle velocity on the global axis without any mitigating brake action

It is assumed that the vehicle is initially running with a longitudinal speed of 30m/s with zero heading angle. It is also assumed that the lateral speed (3m/s) and yaw rate (100°/s) are the initial state generated from a side impact. Fig. 8 and 9 show the predicted vehicle state trajectories on the heading angle / yaw rate phase plane, and the longitudinal vehicle speed without any mitigating actions. Although the results show that the heading angle almost reaches 360° (which is desirable), its lateral deviation is over 20m. So, the lateral displacement needs to be reduced with proper control actions. In Fig. 10, the effects of different braking control actions in the phase plane are shown. Since the tire forces are affected significantly by the wheel slip ratio, the vehicle yaw rate and heading angle are quite different for the three braking actions.

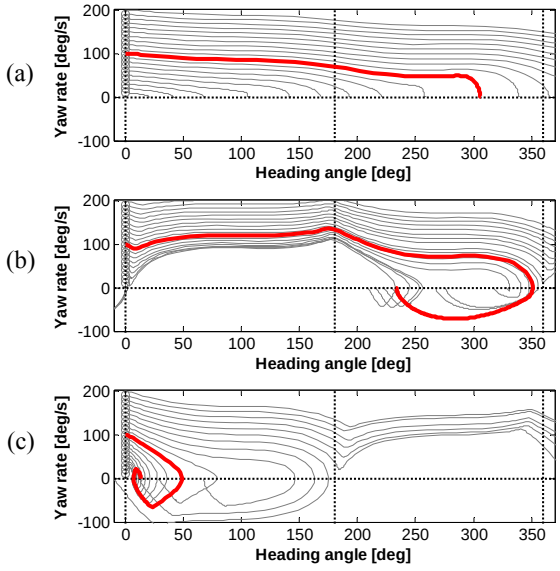


Fig. 10. Comparison of braking actions with the initial state $V_X$ =30m/s and $\omega_z$ =100°/s. (a) 4wheel brake lock. (b) Rear 2wheel brakes lock. (c) Front 2wheel brake lock.

## 4. CONTROL SIGNALS WITH THE OPTIMIZER

### 4.1 Optimization Problem

A gradient descent approach is used to find possible control signals to balance between minimum lateral deviation and safe heading angle. The MATLAB's toolbox (the routine 'fmincon') is used for this constrained optimization problem. The objective function is chosen to minimize lateral deviation while achieving desirable heading angles with the following form:

$$J = \left( w_1 \cdot \sum_{i=1}^{N} \left( Y_s(i) - Y_p(i) \right)^2 + w_2 \cdot \sum_{i=1}^{N} \left( \pi - \psi_{\text{mod}}(i) \right)^2 \right)^{1/2} \quad (16)$$

where $Y_s$ is the lateral displacement from the Earth-fixed X axis, $Y_p$ is the lateral road center position with respect to the Earth-fixed X axis, $\psi_{\text{mod}}$ is the modulo operation of heading angles with $\pi$ ($\psi_{\text{mod}} = \text{mod}(\psi, \pi)$), and $w_1$, $w_2$ are weighting factors.

The objective function is composed of two terms. The equation sums up the square of lateral deviations from the course and sums up the square of angle differences toward to the multiples of 180° along the time span. As the objective function gets minimized, the lateral deviations get decreased and, at the same time, the heading angles get approached to multiples of 180°. A "trade-off" between small lateral deviations and the safe heading angles can be made by adjusting the weights on each term in the objective function. Sequential control inputs, which are longitudinal slip ratios of each tire, are found so that the objective function can be minimized under the slip ratio range constraints:

$$\min_{\lambda_f, \lambda_r} J(\lambda_f, \lambda_r) \quad \textit{subject to} \quad -1 \le \lambda_f, \lambda_r \le 0 \quad (17)$$

Here, we assume that the tire forces are algebraic functions of these tire slip ratios.

### 4.2 Simulation Results

The results in this section show possible brake control actions performed by the optimization scheme under the same vehicle condition in Fig 8-9. In this simulation, all measurements such as position, speed, yaw rate, and heading angle are assumed to be available and accurate, and no actuator dynamics are included in the simulation model. Fig. 11 and Fig. 12 show an example of a trade-off between the lateral displacement and the heading angle with different weighting factors. The result in Fig. 11 achieves 180° heading angle with one lane offset from the course, while the weighing factors in Fig. 12 brings the vehicle to the original lane with 360° turn. So, if the vehicle is free from the secondary collision at least during spinning to 360°, the result in Fig. 12 will be preferred. On the contrary, if the vehicle is expected to have a secondary collision during spinning, keeping the angle to 180° as the trajectory in Fig. 11 might be safer than exposing the side of the vehicle to the collision.

Typically, vehicle stability control actions try to reduce vehicle states quickly. However, if fast stabilizing control action results in a final heading angle of, say, 90°, the vehicle exposes its side to approaching vehicles. In this case, allowing a larger yaw rate may be the right thing to do. Also, if larger yaw rate results in small lateral deviation, it is also desirable. Therefore, it can be seen that this optimization might sometimes produce results against common intuition.

If the host vehicle or the infrastructure can acquire information about the surrounding vehicles, a beneficial heading angle among 0, 180, or 360° (or multiples of

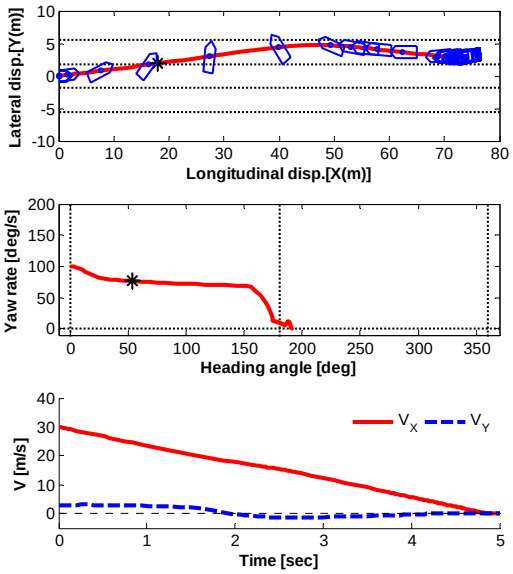


Fig. 11. Projected vehicle position on the road and yaw motion with weightings $w_1 = 100,\ w_2 = 10$

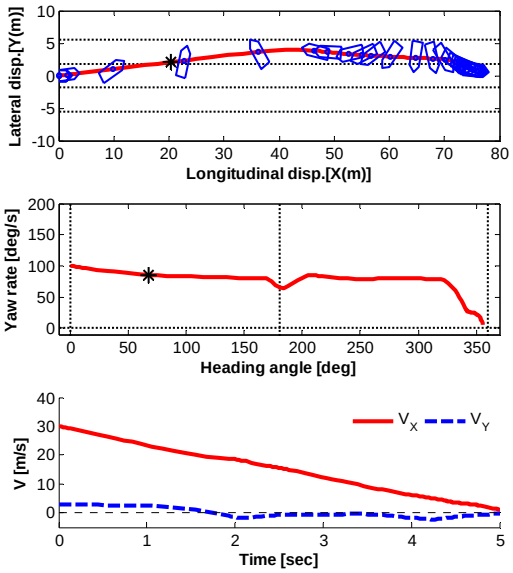


Fig. 12. Projected vehicle position on the road and yaw motion with weightings $w_1 = 100,\ w_2 = 0.1$

180° thereafter) could be determined. For example, if the environmental sensor indicates a possible crash near 60m downstream from the initial (primary) crash, the control action in Fig. 12 is not a good choice. Instead, the vehicle trajectory shown in Fig. 11 is preferred.

## 5. CONCLUSIONS

In this paper, impact force and motion prediction algorithms were developed based on a 4DOF vehicle model. A crash impact strength projection algorithm that estimates the impact and vehicle motion before the crash ends were presented. A constrained minimization problem is formulated which allows a trade-off between small lateral deviation and safe heading angle.

Simulation results show that the combination of different braking actions can lead a vehicle to a desired heading angle and reduce the lateral deviation from the original (unmitigated) trajectory. Studies on the combination of weighting factors and the development of a feedback control algorithm are ongoing works.

## REFERENCES


[1] NHTSA. "Traffic Safety Facts 2009," DOT HS 811 402, 2010.

[2] Zhou, J. "Active Safety Measures for Vehicles Involved in Light Vehicle-to-Vehicle Impacts," Ph. D. Dissertation, University of Michigan, Ann Arbor, 2008.

[3] Langwieder, K., Sporner, A., and Hell. W. "RESICO – Retrospective Safety Analysis of Car Collisions Resulting in Serious Injuries," GDV 9810, Munich, Germany, 1999.

[4] NHTSA. "Problem Definition for Pre-Crash Sensing Advanced Restraints," DOT HS 811 114, 2009.

[5] Piao, J., and Mcdonald, M. "Advanced Driver Assistance Systems from Autonomous to Cooperative Approach," Transport Reviews, vol.28, p.659, 2008.

[6] Dang, J. N. "Preliminary Results Analyzing the Effectiveness of Electronic Stability Control (ESC) Systems," DOT HS 809 790, 2004.

[7] Chan, C.-Y., and Tan, H.-S. "Feasibility Analysis of Steering Control as a Driver-Assistance Function in Collision Situations," IEEE Trans. On Intelligent Transportation Systems, pp. 1–9, 2001.

[8] Robert Bosch GmbH. "Secondary Collision Mitigation," from http://www.bosch.com

[9] Yang, D., Gordon, T., et al. "Post-Impact Vehicle Path Control by Optimization of Individual Wheel Braking Sequences," Proc. of AVEC 2010, pp 882-887

[10] Yang, D., Gordon, T., et al. "Optimized Brake-based Control of Path Lateral Deviation for Mitigation of Secondary Collisions," Proc. of the Institution of Mechanical Engineers, Part D: Journal of Automobile Engineering, vol. 225, no. 12, pp. 1587-1604, 2010.

[11] Zhou, J., Peng, H., and Lu, J. "Collision Model for Vehicle Motion Prediction after Light Impacts", Vehicle System Dynamics, 46, 1, pp. 3-15 2008.

[12] Zhou, J., Lu, J., and Peng, H. "Vehicle stabilization in response to exogenous impulsive disturbances to the vehicle body," In Proc. of the American Control Conference, St. Louis, MO, pp. 701-706, 2009,

[13] Huang, M. "Vehicle Crash Mechanics", CRC Press, Boca Raton, FL 2000.

[14] Hac, A., et al. "Estimation of Vehicle Roll Angle and Side Slip for Crash Sensing," SAE Technical Paper 2010-01-0529.

[15] Pacejka, H. B. "Tire and Vehicle Dynamics (Second edition)", SAE International, 2005.

[16] Mechanical Simulation Corporation. http://www.carsim.com